Using ground penetrating radar to quantify changes in the fracture pattern associated with a simulated rockburst experiment

by M. Grodner*

Synopsis

Ground Penetrating Radar (GPR) is an electromagnetic geophysical reflection technique that maps reflections associated with a change in electric properties of the target medium. It can thus be used to map the geometry of geological features and fractures as these can have different electromagnetic properties to intact rock. GPR was used successfully to determine the position and nature of the fractures in the tunnel sidewall, in the area of the simulated rockburst experiment. By comparing the radar scans acquired before with those acquired after the blast, it was possible to determine which fractures were reactivated by the blast and where new fractures were developed. It was found that the mining-induced fractures that formed during the development of the tunnel were re-activated by the simulated rockburst, as indicated by their increased reflectance on the radar scans. In addition, several new tunnel sidewall parallel fractures developed in the area of the blastholes. GPR thus clearly shows how and where the fracture pattern changed as a result of the blast and contributed to the understanding of the mechanisms of damage associated with the blast, and perhaps rockbursts in general.

Introduction

Ground Penetrating Radar (GPR) is a geophysical technique that provides information based on the target's electrical properties. An electromagnetic pulse is transmitted into the target (e.g. the rockmass) via an antenna (Figure 1). This pulse reflects off an area of dielectric contrast (e.g the air-rock interface of the fracture f-f). This reflected wave (dashed radiating pattern) is picked up by the antenna. Information including it's arrival time and strength are recorded by the Data Acquisition Unit (DAU) and transferred to a PC for conversion to a radargram. Any interface between materials, in the target area, with different dielectric properties will reflect back (to a greater or lesser extent) the pulse to the receiver antenna and thus allow the position of this interface to be determined. Fractures in the rockmass are strong dielectric interfaces (because of the presence of air in an otherwise solid target area) and thus GPR can be used to determine the extent of fracturing around an excavation, even though it may not be possible to resolve individual fractures. The higher the frequency of the transmitted waves the smaller the feature that can be resolved. Unfortunately higher frequencies cannot penetrate as far, and thus it is important to understand the size and type, as well as the depth of the target. The output from a radar scan is a radargram which is a two-dimensional slice of the reflected signal strength in a plane. These differences in the reflection can then be interpreted as particular fractures by using additional geotechnical information such as fracture mapping and petroscope observations.

Method

As part of the investigations into the change in rockmass characteristics associated with the simulated rockburst, several GPR scans were conducted into the tunnel sidewall at the simulated rockburst site. GPR scans were conducted by moving the antenna along the tunnel sidewall in the area of interest (see Figure 2). Eight GPR scans were measured before, and seven after the simulated rockburst. It was anticipated that the radar scans would at least qualitatively show an increase in the fracturing around the area of the blast and in the vicinity of the tunnel wall. Each set of radar scans took two persons less than 2 hours to complete, once again highlighting the ease of use of the GPR system.

The radar scans were acquired using the SIR2M radar system, with a 500 MHz antenna attached. Different range settings were selected to produce the appropriate depths of penetration. These range settings varied from 35 ns to 150 ns, which with a 500 MHz

* *CSIR: Division of Mining Technology, Auckland Park, South Africa.*

 Paper received Feb. 2001; revised paper received Aug. 2001.

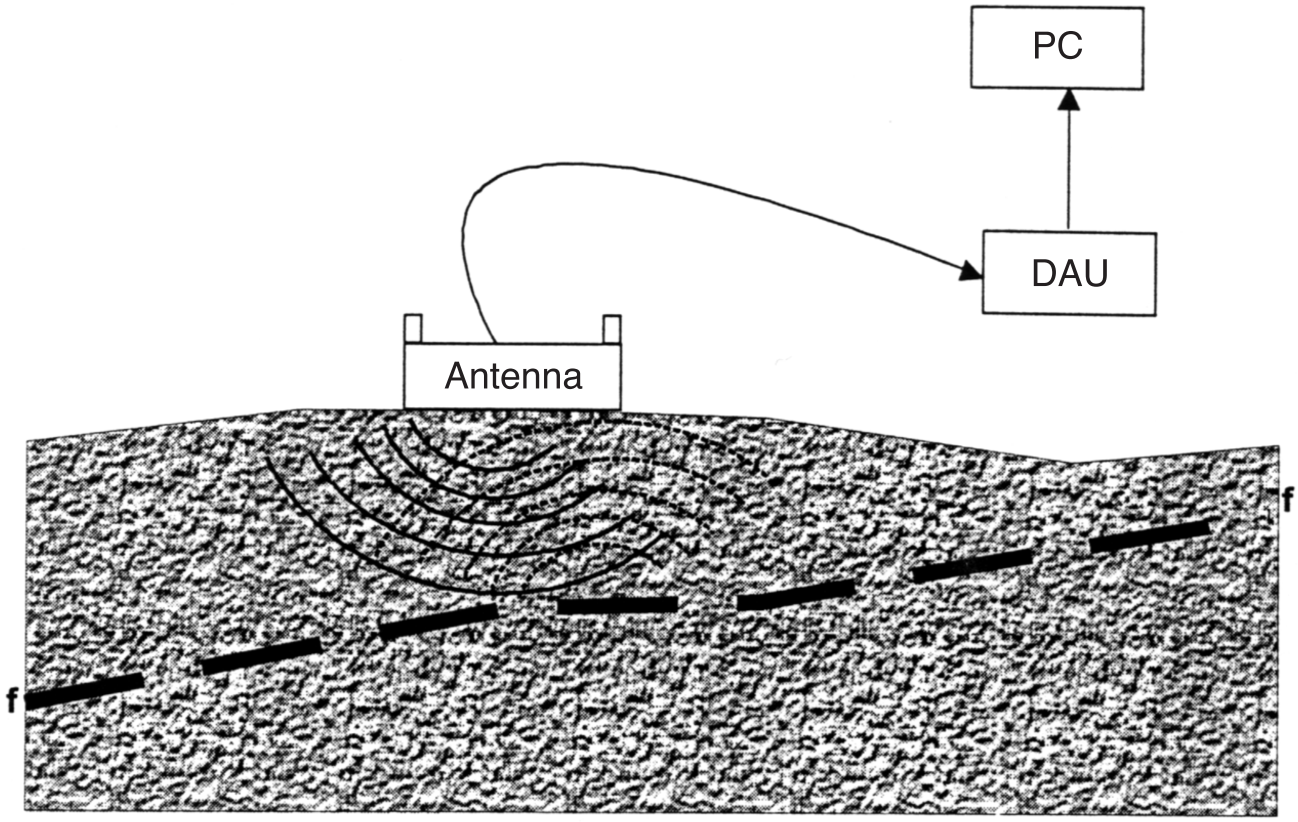

Figure 1—Sketch diagram showing the principle of GPR (see text for further details)

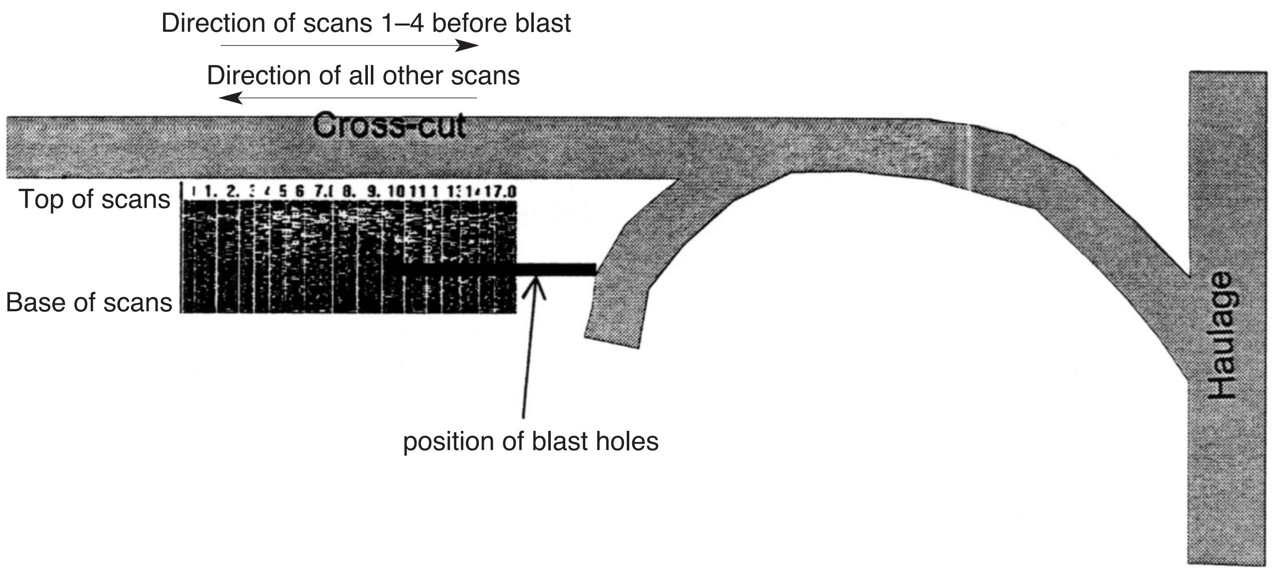

Figure 2—Plan showing orientations of all radar scans

antenna equates to a depth of penetration of between 2.5 m and approximately 9 m. It should be appreciated that although the lower range settings do not give as high a penetration, they have much higher resolution.

Although fractures typically have a high dielectric contrast with the intact rock mass, there are several obstacles in an underground situation that also have high dielectric contrasts and can thus potentially interfere with the electromagnetic signal. It was anticipated that the rock bolts in the tunnel sidewall would interfere with the scans, as they are strong electromagnetic reflectors. It was possible however, in most cases to avoid the bolts during the scan. Even when the antenna was dragged across the bolts, there was very little interference, because of the small cross-sectional area of the bolt that was exposed to the radar signal. It was also expected that the steel pipes placed in the tunnel to anchor the drill machine would interfere with the radar signal. This was indeed the case, but the reflections caused by the pipes were easily recognized and thus ignored on the radargram during interpretation. The effect of the radar cable, ringing and airwaves along the tunnel sidewall was also seen in several of the radargrams but once again these were readily recognized and therefore ignored during the analysis of the data.

Results

Figure 2 shows the orientation of all the radar scans relative to the tunnel sidewall. Only selected scans, which illustrate key points, are shown in this paper. The radargrams were processed using RockPulse 2. The processing history of all the files was simple and the same, thus eliminating the probability of processing artifacts appearing in certain scans. It also allowed the direct comparison of the different scans. A vertical filter (high = 20 MHz, low = 55 MHz) was applied to the data to take out the noise associated with scatter from the tunnel sidewall. A horizontal boxcar filter (length = 30 MHz) was also applied to the data to remove any parallel artifacts.

Pre-experiment GPR scans

Eight GPR scans were taken along a 24 m long section of the tunnel, with the projected area of the blast being in the centre of this section. Four scans were taken in either direction to see if there was any difference in the signal when the radar system was initialized at different ends of the area of interest. Even though it appeared that there were differences in the data during collection, it was found that there was very little difference in the processed radargrams.

A well-defined band of reflection that extends into the sidewall to a depth of approximately 4.5 m can be seen in the different scans. Scan 4 (150 ns range) demonstrates that this band does not extend beyond approximately 4.5 m (Figure 3). At higher range settings, such as with scan 4, there is generally very little reflection from the first part of the scan and hence it appears as though there is no fracturing near the edge of the tunnel. This was one of the reasons that the radar scans were conducted at several different range settings. On several of the scans, the orientation of the mining-induced fractures that formed during the development of the tunnel can be clearly seen (Figure 3).

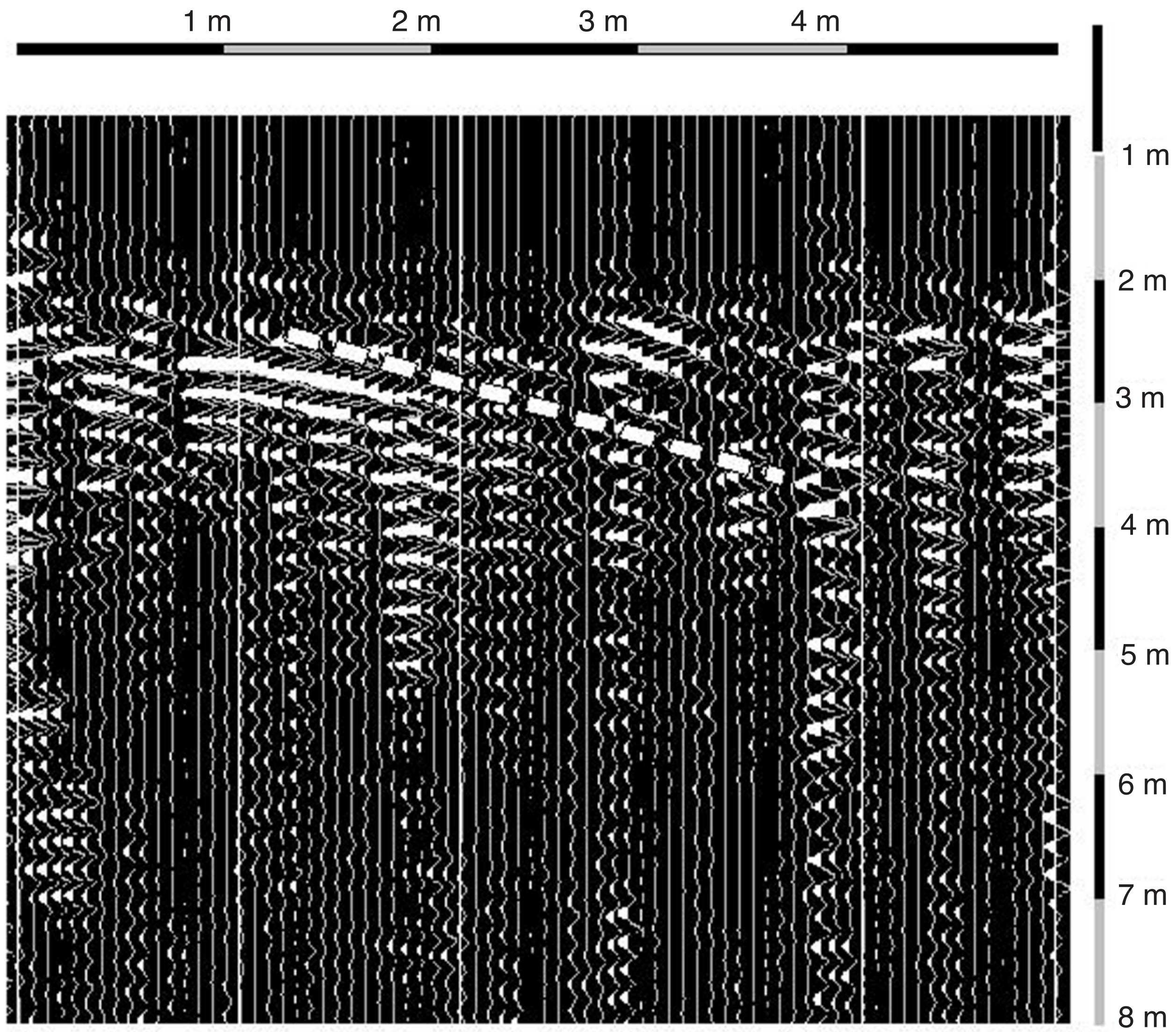

Figure 3—Part of scan 4 (before blast). The dotted line indicates the orientation of the oblique mining-induced fractures. Direction of tunnel development is from right to left

Post-experiment GPR Scans

Seven GPR scans were taken after the simulated rockburst experiment. Due to the fact that there were no major differences in the scans taken in either direction before the blast, it was decided to conduct all the post-blast scans in the same direction. As the paint marks from the previous survey were still visible in places it was possible to conduct the scans over the same area, thereby allowing direct comparison between the two sets of results. Unfortunately the quality of the data in the post-blast scans was not as good as that of the pre-blast scans, probably due to poor coupling with the sidewall. The poor coupling was most likely a result of the extensive amount of loose rock on the tunnel sidewall, which inhibited penetration of the radar signal. As such only selected post-blast scans are shown and compared to the equivalent pre-blast scans. Post-blast scans 3 and 7 did however provide reasonable results. These scans are the 'after' scans in Figures 6a and 6b. There are several well-defined reflectors at a depth of between 3 m and 6 m, which do not appear on the pre-blast scans (Figures 4 and 5). It is suggested that these are fractures that either formed as a result of the blast or were extended by the blast.

Comparison of before and after blast results

As the GPR scans were taken over the same section of tunnel sidewall it is possible to directly compare the pre- and post-blast results. Following the blast there is a noticeable increase in the intensity of fracturing in the tunnel sidewall.

Figures 6a and b show the mining-induced fractures on the pre- and post-blast scans. In the post-blast scans there is an increase in the overall intensity of the reflections of the mining-induced fractures. This is probably a combination of two factors, firstly the gain, which is set automatically by the radar system, was higher for the post-blast scans and secondly there probably was a real increase in the amount of fracturing. As mentioned previously this could be due to the development of new fractures and/or the extension of pre-existing ones.

In addition to the reactivation and extension of the fractures near the tunnel sidewall, there was also the development of several tunnel parallel fractures at the approximate depth of the blast-hole fan. These fractures are

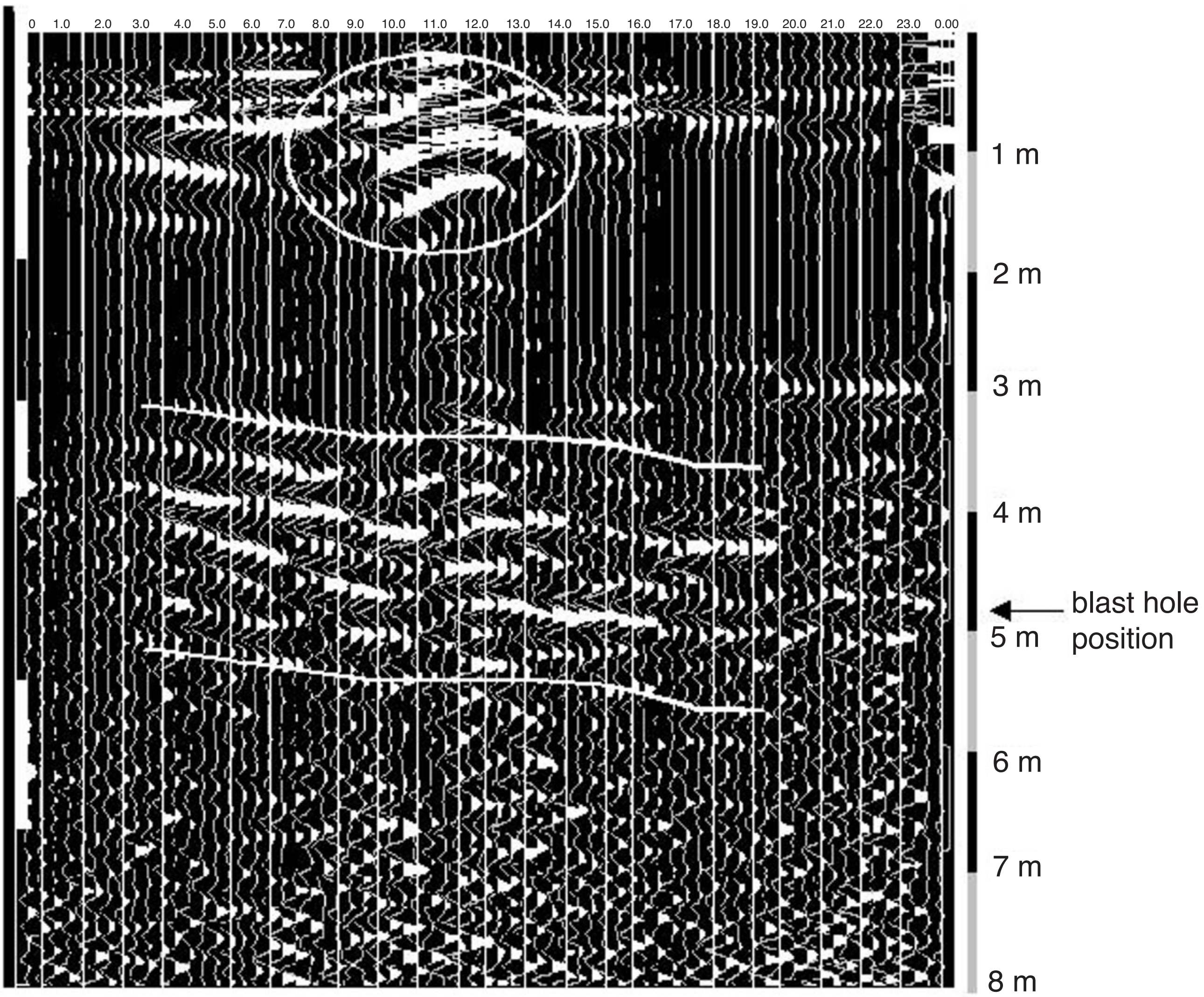

Figure 4—Scan 3 (after the blast) of the same area as Figure 3. The dilation of the sidewall parallel opposite the area of the blast (circle) and the development of deeper fractures between the parallel lines) at between 3 m and 6 m can be seen. The arrow indicates the position of the blasthole fan

most likely to be steeply dipping, as shallowly dipping fractures would not reflect the radar signal well and would thus not be clearly visible on the radargram. It is interesting to note that there is not a single fracture surface but rather an anastomosing (branching) fan of fractures (Figure 5). The shape of this fan is consistent with a blast that propagated towards the end of the tunnel (from right to left in Figures 4 and 5).

Summary and conclusions

GPR provided an 'insight' into the changes that occurred to the rock mass between the blast-hole fan and the tunnel sidewall. The scans provided a reasonably complete picture of the nature of the fracture pattern that could be used in the interpretation of the other data collected from the site. Although the quality of the data (especially of the post-blast fracturing) was not as good as was hoped, it is still possible to discern a change in the fracture pattern. This can be summarized as follows: the amount of dilation on the pre-existing mining-induced ('bow-wave') fractures was increased by the blast, whilst deeper into the sidewall it appears as though several sidewall parallel fractures were developed in the vicinity of the blast holes. These findings confirm the notion that much of the damage due to rockbursts is dependent on the pre-existing flaws in the rock mass. The fact that failure and slip does not have to occur on a single plane is also highlighted by the discovery of multiple fracture surfaces in the area of the blast-holes.

Some of the limitations of GPR were also highlighted during this study and it is important to bear these in mind. Any given technique cannot provide all the answers and should be used in conjunction with complementary methods. Firstly the poor coupling of the radar signal through the broken rock (and the associated autogain adjustments) led to many of the post-blast scans being uninterpretable. Secondly

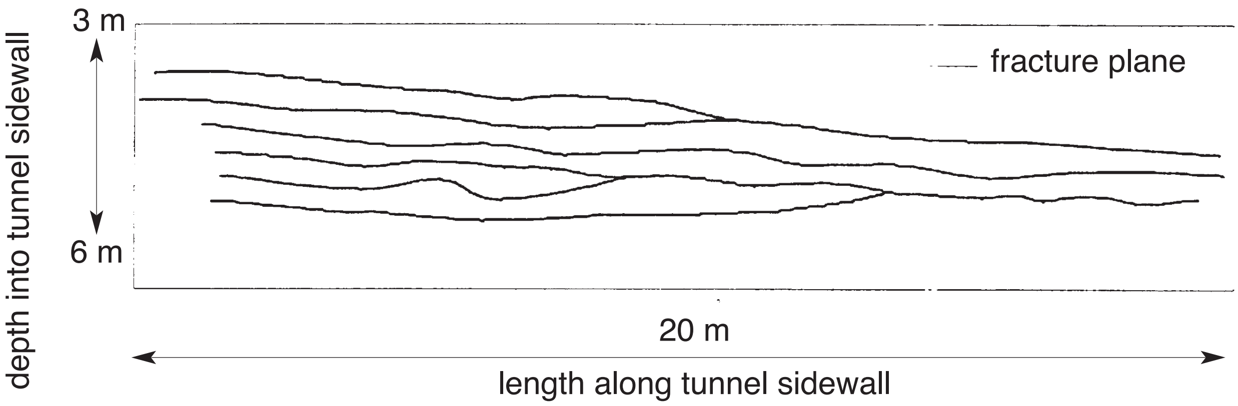

Figure 5—Interpretation of radargram shown in Figure 4, indicating the anastomosing nature of the tunnel parallel fractures formed in the vicinity of the blast-hole fan. The blastholes were drilled in fan 5 m from the tunnel sidewall

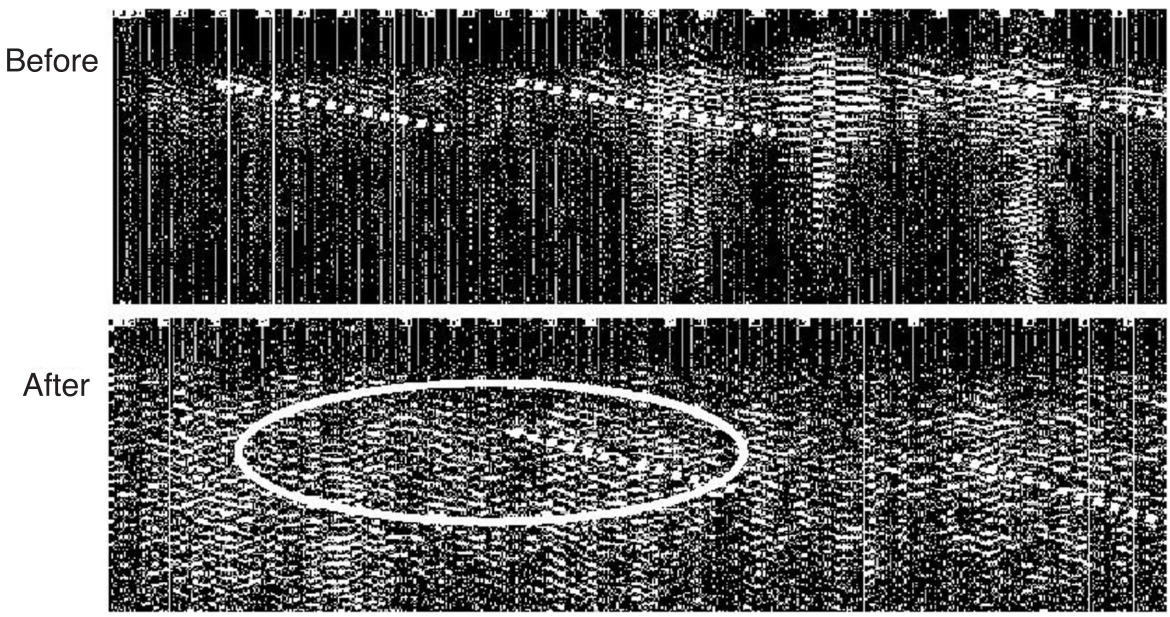

Figure 6a—Comparison of radar scans from before and after the simulated rockburst (100 ns range setting—depth of penetration approximately 7.5 m). The dotted lines indicate the orientation of the mining-induced fractures and the circle the area of the controlled blast. Note there is some loss of quality due to rotation of the image into the correct orientation for publication

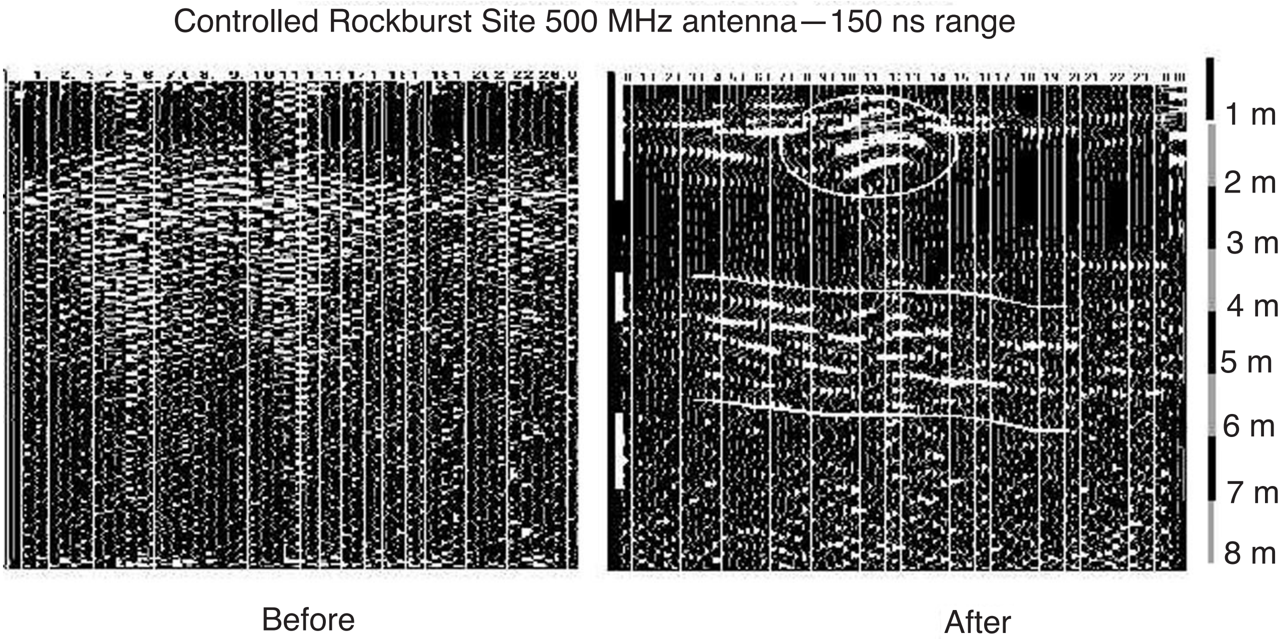

Figure 6 b—Comparison of radar scans from before and after the simulated rockburst (150 ns range setting—depth of penetration approximately 11 m). Note lack of well-defined reflectors at approximately 6 m depth in the before blast scan

the best reflections are obtained from fractures orientated perpendicular to the direction of propagation of the radar wave, as these provide the strongest reflections. Thus even though the reactivated mining-induced fractures and the fractures in the immediate vicinity of the blast hole were seen, it is possible that there are additional fractures perpendicular to the tunnel sidewall that would not be distinct on the radargram. ◆

GeoInside starts online trading in mineral commodities*

Berlin, April 13th, 2001. The Business-to-Business Market Place operator GeoInside is expanding its service. GeoInside offers on its Website, www.GeoInside.com, a trading platform for mineral commodities to mine operators, processors, agents and buyers.

The core business of GeoInside is a moderated matchmaking between supply and demand. Via the GeoInside Website, buyers and sellers can anonymously present their sales and supply requests, exchange information via Internet, Fax, Phone, and finally make personal contacts or visits. GeoInside monitors the matchmaking process between business partners and gets a commission after successful completion of a deal. As GeoInside takes an independent market position, it is able to provide frank and fair information about products and business partners.

Small- to medium-scale mining and processing companies in particular benefit from the Internet and can enhance their market position through online trading. The first mineral commodity sales offers are, for example, for tantalite, chromite, vermiculite, bentonite, mineral pigments, natural stones and gemstones. Trading has now started and several transactions have successfully been completed. GeoInside provides samples, assists in controlling the quality, arranges transport, and guarantees payment to the seller. GeoInside also visits mine operators as well as the interested buyers, thus being able to give valuable recommendations for the trade.

GeoInside also helps to streamline the transport of mineral commodities to make mineral products more competitive and trading more economic. On request, GeoInside can also carry out exploration, mining and processing consultancies, or can advertise tenders for such services.

Apart from the trade in mineral commodities, the Market Place includes the invitation for tenders for private and public sector projects in the field of earth sciences. A job market and product catalogue complement the information and trading platform.

GeoInside is directed by two geologists, Dr Peter Hanstein and Dr Peter Buchholz, who have over 10 years experience in mineral commodities and management of international projects. The head office is located in Berlin, Germany, with branches in Zimbabwe and Brazil. ◆

* *Issued by: GeoInside GmbH, Dr Peter Hanstein, Info: www.GeoInside.com, Email: Peter Hanstein@ GeoInside.com, Tel: +49 30 8862862 0, Fax: +49 30 8862862 1*